

We are IntechOpen, the world's leading publisher of Open Access books Built by scientists, for scientists

6,900

Open access books available

186,000

International authors and editors

200M

Downloads

Our authors are among the

154

Countries delivered to

TOP 1%

most cited scientists

12.2%

Contributors from top 500 universities



WEB OF SCIENCE™

Selection of our books indexed in the Book Citation Index
in Web of Science™ Core Collection (BKCI)

Interested in publishing with us?
Contact book.department@intechopen.com

Numbers displayed above are based on latest data collected.
For more information visit www.intechopen.com



Hydrothermal Synthesis of Zinc Tin Oxide Nanostructures for Photocatalysis, Energy Harvesting and Electronics

Ana Isabel Bento Rovisco, Rita Branquinho, Joana Vaz Pinto, Rodrigo Martins, Elvira Fortunato and Pedro Barquinha

Abstract

The massification of Internet of Things (IoT) and Smart Surfaces has increased the demand for nanomaterials excelling at specific properties required for their target application, but also offering multifunctionality, conformal integration in multiple surfaces and sustainability, in line with the European Green Deal goals. Metal oxides have been key materials for this end, finding applications from flexible electronics to photocatalysis and energy harvesting, with multicomponent materials as zinc tin oxide (ZTO) emerging as some of the most promising possibilities. This chapter is dedicated to the hydrothermal synthesis of ZTO nanostructures, expanding the already wide potential of ZnO. A literature review on the latest progress on the synthesis of a multitude of ZTO nanostructures is provided (e.g., nanowires, nanoparticles, nanosheets), emphasizing the relevance of advanced nanoscale techniques for proper characterization of such materials. The multifunctionality of ZTO will also be covered, with special attention being given to their potential for photocatalysis, electronic devices and energy harvesters.

Keywords: hydrothermal synthesis, zinc tin oxide, nanostructures, nanowires, multifunctionality, sustainability

1. Introduction

Nanotechnology attracted wide attention over the last decades, leading to a very fast development of materials and processing routes. Different areas such as electronics, cosmetics, medicine/biology, optical systems, energy, and many others, have profited from this rapid growth. Having in mind the environmental issues that we are facing in the modern era, the importance of searching for environmentally friendly, recyclable and low cost nanomaterials and fabrication processes is essential [1].

This has been a concern in strategic areas as large area electronics (LAE), one of the fastest growing technologies in the world, with projected market growth from \$31.7 billion in 2018 to \$77.3 billion in 2029 [2]. LAE includes many segments (e.g., displays, sensors, logic, memory), which are desired to be seamlessly integrated on virtually any object to create smart surfaces. Due to their good electrical properties, transparency, large area uniformity and good mechanical flexibility, oxide thin

films have been crucial materials to advance these concepts [3]. Depending on the metal cations (and on the metal to oxygen ratio), metal oxide thin films can be considered as dielectrics, semiconductors or even conductors [4–6]. Owing to their remarkable electrical properties, In-based materials, such as ITO (indium tin oxide) and IGZO (indium-gallium-zinc oxide) are currently the multicomponent oxide conductor and semiconductor thin films with larger market relevance in LAE [4, 7]. However, indium is an expensive material, due to its scarcity and high market value, appearing in the current list (2020) of the critical raw materials from the European Commission [8]. The same applies for gallium, another element of IGZO. Therefore, the replacement of these materials is imperative to assure long-term sustainability [1].

This quest for new oxide materials is naturally also transposed for nanostructures, as their fascinating properties will certainly boost even further the demand for oxide (nano)materials in a plethora of industries. Departing from critical cations, ZnO is perhaps the most widely studied oxide nanostructure. Its properties are nowadays well-known and useful for multiple applications, from photocatalysis, to solar cells or biosensors [9]. It can also be prepared by a multiplicity of methodologies, from vapor- to solution-based processes [10]. Multicomponent oxide nanostructures, particularly those based on sustainable materials, have been significantly less studied, but already show great potential to enhance properties and enlarge the range of applications of oxides. As in thin films, a great advantage of these multicomponent materials is the possibility of tuning their properties by adjusting the cationic ratio [11, 12]. Zinc tin oxide (ZTO) is one of the multicomponent oxides that has been explored and has shown very interesting properties when compared with its binary counterparts (ZnO and SnO₂). In fact, ZTO was already demonstrated to exhibit similar properties to IGZO in low-temperature thin film transistors (TFTs), while avoiding the use of critical raw materials [13].

This chapter provides a literature review on the hydrothermal synthesis of ZTO nanostructures, the main properties of this material, and its applications, highlighting its multifunctionality.

1.1 Hydrothermal synthesis of ZTO nanostructures

Hydrothermal methods have been widely explored and developed in the last years [14]. This method consists in a chemical reaction in an aqueous solution, under high pressure (> 1 atm) and at temperatures usually ranging between 100°C and 300°C. In case of using non-aqueous solvents, the method is called solvothermal. Typically, the solution is kept inside an autoclave and a conventional oven is used as heat source. The pressure inside the autoclave is dependent both on the temperature and the volume used. This allows for a high energy supply for the reactions even at relatively low temperatures. While the typical nucleation and growth mechanism of the oxide nanostructures in these reactions is thought to consist mainly in dissolution–reprecipitation, these mechanisms are often not well understood.

The synthesis of multicomponent oxide materials such as ZTO is usually easier and more efficient by vapor phase methods, such as chemical vapor deposition and thermal evaporation, than by solution processes, due to the higher temperatures of the former. However, vapor phase methods present drawbacks that are important to consider, such as high temperatures (>700°C) and high costs. On the other hand, while inexpensive and simple, the hydrothermal technique still allows for a well-controlled synthesis of the desired nanostructures' shape and structure with high reproducibility, thus presenting as an excellent alternative to the conventional physical methods [15, 16]. Additionally, while conventional ovens are typically used

as the heat source, microwave-assisted synthesis started recently to be widely explored, enabling reduced synthesis duration due to its more efficient and more homogeneous heat transfer process [17].

1.2 Overview on ZTO nanostructures produced by hydrothermal synthesis

ZTO appears commonly in two main forms, a stable one, Zn_2SnO_4 , and ZnSnO_3 , a metastable phase. The stable Zn_2SnO_4 phase is an orthostannate with an inverse spinel structure and is a n-type semiconductor with a band gap of 3.6 eV [18]. ZnSnO_3 , the metastable phase, can have a rhombohedral structure or a perovskite structure either orthorhombic (–orth) or ordered face centered structure (–fcc) [14, 19]. This phase is a well-known piezo/ferroelectric material and presents a band gap of 3.9 eV [18]. Several ZTO nanostructures such as nanoparticles, octahedrons, nanocubes, nanowires, and nanoflowers, have been produced by hydrothermal synthesis, appearing in both ZnSnO_3 and Zn_2SnO_4 phases. **Figure 1** shows examples of Zn_2SnO_4 and ZnSnO_3 nanostructures with different morphologies and dimensions (0D, 1D, 2D and 3D) produced by hydrothermal synthesis.

Lehnen *et al.*, for example, reported very small Zn_2SnO_4 quantum dots (with diameters below 30 nm), produced with a microwave-assisted hydrothermal synthesis, followed by high-temperature annealing [20]. Numerous other reports on Zn_2SnO_4 nanoparticles have been shown (**Figure 1a**), either using standard hydrothermal synthesis or solvothermal synthesis [16, 21–28]. Regarding ZnSnO_3 nanoparticles (**Figure 1b**), several hydro and solvothermal routes have been reported for its synthesis [29–32]. For instance, Beshkar *et al.* reported the use of the Pechini method at 80°C to synthesize fcc- ZnSnO_3 nanoparticles, followed by a calcination at 700°C for 2 h [33].

Concerning 1D structures, while several reports on Zn_2SnO_4 nanowires exist, these consist essentially in vapor phase methods, more specifically in thermal evaporation at high temperature (>750°C) [19], showing the difficulty in obtaining the stable phase of ZTO in the nanowire form [34]. This is emphasized by the fact that there are only a few reports for Zn_2SnO_4 nanowires from hydrothermal synthesis, mostly assisted by seed-layers. For example, Zn_2SnO_4 nanowires were grown on a stainless steel seed-layer and from Mn_3O_4 nanowires [35, 36]. Zn_2SnO_4 nanorods by hydrothermal synthesis were also reported by Chen *et al.* (**Figure 1c**), but only organized in 3D flowerlike superstructures [37]. Regarding ZnSnO_3 , only a few reports for nanowires exist, also consisting typically in physical processes (carbon-thermal reaction, thermal evaporation or CVD processes) [38, 39]. For hydrothermal processing of ZnSnO_3 nanowires seed-layers are typically used. Lo *et al.* employed an FTO thin film as seed-layer for this end (**Figure 1d**) [40–42]. A different approach was reported by Men *et al.* who transformed ZnO nanowires into ZnSnO_3 nanowires by a hydrothermal synthesis [41]. Recently, our group demonstrated for the first time ZnSnO_3 nanowires obtained by an one-step hydrothermal synthesis without employing any seed-layer (**Figure 1e**) [32, 43].

2D structures of ZTO have also been reported. Joseph *et al.* synthesized fcc- ZnSnO_3 flakes by a hydrothermal method at only 100°C [44]. Guo *et al.* produced orth- ZnSnO_3 nanoplates (**Figure 1f**) by a hydrothermal process at 260°C for 24 h [45]. Chen *et al.* obtained orth- ZnSnO_3 nanosheets through a hydrothermal synthesis at 180°C for 12 h, where a precipitate of $\text{ZnSn}(\text{OH})_6$ was achieved followed by a calcination at 600°C for 3 h [46]. Zn_2SnO_4 nanoplates have also been reported, for example, by Cherian *et al.* (**Figure 1g**) [34].

There are also several reports regarding 3D ZTO nanostructures. Gao *et al.* reported the synthesis of ZnSnO_3 hollow spheres (**Figure 1h**) by hydrothermal synthesis at 120°C for 3 h [47]. A commonly reported shape for ZTO nanostructures

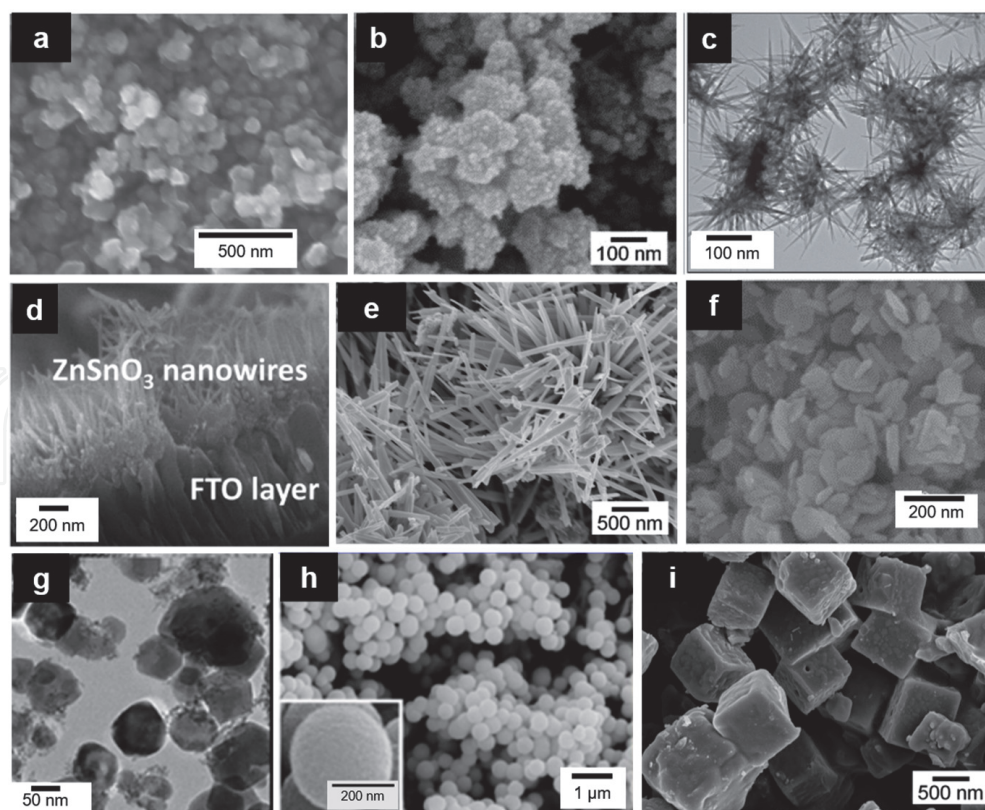


Figure 1.

Multiple ZTO nanostructures obtained by hydrothermal synthesis, analyzed by scanning electron microscopy (SEM): (a) Zn_2SnO_4 nanoparticles, from reference [28]; (b) fcc- $ZnSnO_3$ nanoparticles produced by our group; (d) rhombohedral- $ZnSnO_3$ nanowires growth on FTO seed-layer, reprinted with permission from [42], copyright (2020) American Chemical Society; (e) orth- $ZnSnO_3$ nanowires synthesized without employing seed-layers (in form of powder), from reference [43]; (f) orth- $ZnSnO_3$ nanoplates, reprinted with permission from [45], copyright (2020) American Chemical Society; (h) orth- $ZnSnO_3$ hollow spheres, reprinted with permission from [47], copyright (2020) American Chemical Society; (i) orth- $ZnSnO_3$ nanocubes produced by our group; and by transmission electron microscopy (TEM): (c) Zn_2SnO_4 nanorods, reprinted with permission from [37], copyright (2020) American Chemical Society; and (g) Zn_2SnO_4 nanoplates, reprinted with permission from [34], copyright (2020) American Chemical Society.

is the nanocube shape (**Figure 1i**). For instance, Chen *et al.* reported a synthesis which could result in $ZnSnO_3$ nanocubes or $ZnSnO_3$ nanosheets, depending on the processing temperature [46]. The octahedron shape is also common, and octahedrons of Zn_2SnO_4 have been reported by several groups, being these identified as the most stable phase and shape for ZTO nanocrystals. Zn_2SnO_4 octahedrons constituted by nanoplates can also be formed [48].

While **Figure 1** shows the wide range of possibilities offered by hydrothermal synthesis within the ZTO system, it is challenging to obtain structures with a targeted phase ($ZnSnO_3$ or Zn_2SnO_4 in this case) and shape (e.g. nanosheet or nanowire) [40, 49]. For this end, a comprehensive tailoring of the synthesis parameters is required.

2. Research methods

Usually the hydrothermal synthesis of ZTO nanostructures is performed inside a teflon-lined stainless-steel autoclave using a conventional oven as heating source. Nevertheless, as previously shown, there are already a few examples of microwave-assisted hydrothermal synthesis of ZTO nanostructures. As an example of a typical

method, our synthesis starts with the dissolution of the zinc and tin precursors separately in 7.5 mL of deionized water, followed by their mixture. Then a surfactant (ethylenediamine, EDA) is added, and the solution is magnetically stirred for 30 minutes. The last step is the addition of the mineralizer agent (NaOH). It is observed that milling the precursors before their dissolution in water leads to a more homogeneous result. After the solution preparation, it is transferred into the autoclave and kept in the oven for 24 h at 200°C. After the synthesis, the resultant precipitate (comprising the nanostructures) should be washed several times with deionized water and isopropyl alcohol, alternately, and centrifuged at each time. The nanostructures are usually dried at $\approx 60^\circ\text{C}$, in vacuum, for a at least 2 hours [32, 43].

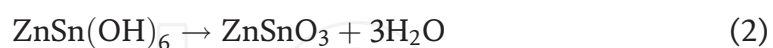
3. Results and discussion

3.1 Growth mechanism of ZTO nanostructures

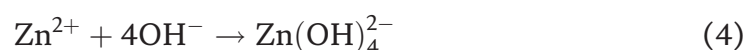
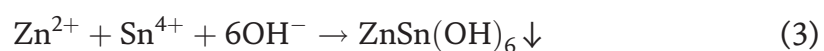
3.1.1 Tailoring the chemico-physical parameters of the hydrothermal synthesis

Understanding the influence of each synthesis parameter is a key step in achieving the desired structures. Specifically, considering seed-layer free processes allows evaluation of the intrinsic influence of each synthesis parameter on the nanostructures' growth. Moreover, the solvent also plays a major role in the process strongly determining the dissolution and diffusion of the species during the synthesis. When the precursors' solubility is not high enough, precluding an efficient reaction, mineralizer agents can be used (NaOH, KOH, etc.) to increase the solubility of the species [50, 51].

To understand the growth within Zn:Sn:O system it is essential to revise the main equations related with the chemical reactions behind each ZTO phases. The chemical reaction processes for the formation of ZnSnO_3 nanostructures have been represented in the literature by the following equations [52]:

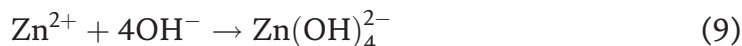
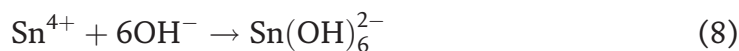


Regarding Zn_2SnO_4 , its formation has been described by different reactions depending on the precursors and solvents involved in the synthesis. For example, Li *et al.* represented the chemical reaction of Zn_2SnO_4 nanowires through the equations below, which have been the most common in literature [35].

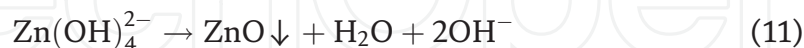


On the other hand, Fu *et al.* employed a different synthesis method to avoid the use of NaOH, using four different amines (surfactants) instead [53], represented as:





Several reports show that ZnO and SnO₂ crystals can co-exist with ZTO nanostructures when the synthesis parameters differ, even if slightly, from the ideal conditions for ZTO formation. Usually the formation of ZnO (Eq. 11) and SnO₂ (Eqs. 12–14) is associated with the two alkaline concentration extremes, higher and lower, respectively [54].



In fact, in our previous work on seed-layer free synthesis of ZTO nanowires, using zinc and tin chloride precursors at a fixed concentration ratio it was shown that while for lower NaOH concentrations SnO₂ nanoparticles were obtained, for higher NaOH concentrations ZnO nanowires (mixed with fcc-ZnSnO₃ nanoparticles) were achieved, whereas intermediate NaOH concentrations yielded ZnSnO₃ nanowires [32]. As shown in **Figure 2**, a similar trend is seen even when increasing only the NaOH concentration (keeping the precursors' concentration fixed). This suggests that there is an optimal concentration of the mineralizer. These results agree with those reported by Zeng *et al.*, [54] however, while the authors suggest specific values of pH for obtaining the different structures (SnO₂, Zn₂SnO₄ and ZnO), in our case the pH is much higher due to the presence of ethylenediamine (EDA) which yields a pH of at least ≈ 12 , showcasing the trend specifically with the variation of the NaOH concentration and not necessarily the overall pH [32].

As mentioned, the precursors' solubility is a key factor to achieve a well-controlled synthesis. Our previous work showed that for different zinc precursors (zinc chloride or zinc acetate), maintaining the same tin precursor (tin chloride), the reaction differs, being slower and less homogeneous when using zinc acetate, due its lower solubility in the EDA surfactant. The use of surfactants, such as EDA, cetrimonium bromide (CTAB) and sodium dodecyl sulfate (SDS), is very common specially when aiming to induce the growth of 1D nanostructures. Surfactants act as



Figure 2. SEM images of resultant nanostructures from synthesis with different precursors' molar concentrations, i.e., ZnCl₂:SnCl₄.5H₂O:NaOH of (a) 2:1:12 M, (b) 4:2:24 M (from reference [43]) and (c) 8:4:48 M, respectively, while maintaining the same proportion between them. Increasing the precursors' molar concentrations the materials obtained follow the common trend when increasing only the NaOH concentration: SnO₂ nanoparticles, orth-ZnSnO₃ nanowires and ZnO nanowires (mixed with fcc-ZnSnO₃ nanoparticles).

directing growth agents as their molecules aggregate to the surface of the metallic atoms inducing the growth of specific structures/shapes. The solubility of each precursor in the solvents is a key factor for achieving a better synthesis efficiency and homogeneity. This also influences the Zn to Sn precursor ratio required to optimize the achievement of the desired nanostructures.

The duration and temperature of the synthesis are also crucial to determine the achieved nanomaterials. Several reports showed that below 180°C no ZTO phases are obtained, with the intermediate phase $\text{ZnSn}(\text{OH})_6$ being produced instead [43, 45]. Zeng *et al.* showed that to obtain Zn_2SnO_4 nanostructures a temperature of at least 200°C and 20 h of synthesis are necessary [54]. Meanwhile, Guo *et al.* observed that 12 h at 260°C are required to produce orth- ZnSnO_3 nanoplates for that specific solution process [45]. In our work on the synthesis of orth- ZnSnO_3 nanowires, it was observed that syntheses with 12 h at 200°C were necessary for a predominant growth of nanowires. However, for very long synthesis, or at higher temperatures (220°C), the decomposition of the ZnSnO_3 phase into the more stable phases starts to occur. It was also concluded that lower energy levels favor the growth of the more energetically stable phases (Zn_2SnO_4 , ZnO and SnO_2), the metastable ZnSnO_3 is achievable for intermediate energy levels, and for higher energy levels the decomposition (into Zn_2SnO_4 and SnO_2) of ZnSnO_3 starts to occur. Higher solution volumes, corresponding to higher pressure in the synthesis, were found to be necessary for obtaining the ZnSnO_3 phase. A general growth mechanism for orth- ZnSnO_3 nanowires and Zn_2SnO_4 nanoparticles was proposed and is shown in **Figure 3** [43].

While tailoring the chemico-physical parameters is always necessary, the use of a seed-layer material, usually a thin film, can be very effective in strongly inducing the growth of a desired structure by means of an epitaxial growth mechanism. This approach is commonly used when 1D structures are aimed, as briefly mentioned in the previous section. The selection of the seed material depends on the desired material and structure (phase and shape) and while several reports for different structures exist, the relation between different seed materials and grown structures was not detailed yet in literature. This depends on a complex interrelation between preferential epitaxial growth and thermodynamical stability of the multiple phases and shapes within the Zn-Sn-O system. While the seed-layer route presents advantages for specific applications such as gate-all-around transistors or photocatalysis [55, 56], its absence also brings numerous benefits. For instance, one of the main

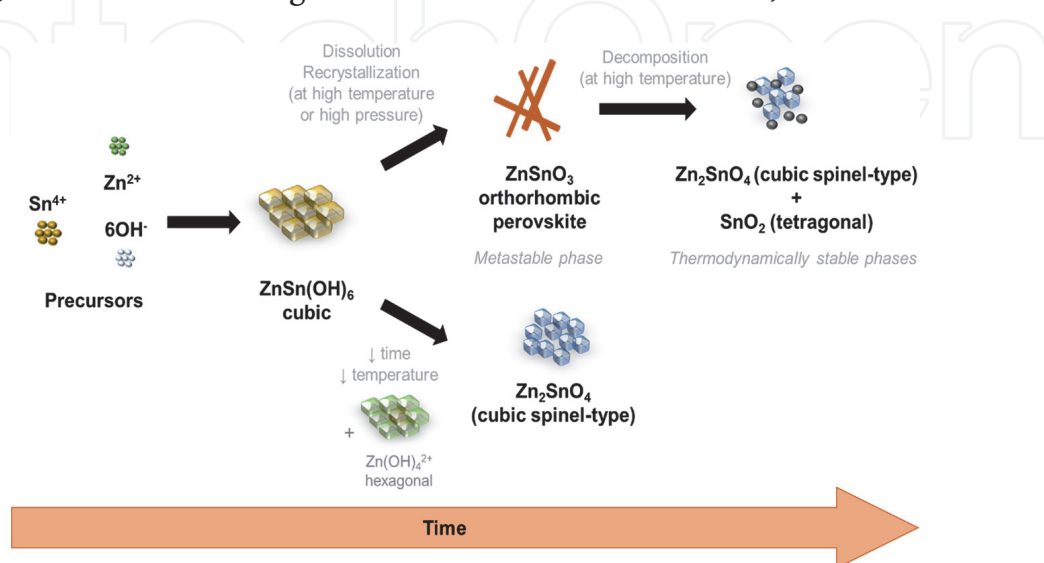


Figure 3. Schematic of the growth mechanism of ZTO nanostructures (ZnSnO_3 nanowires and Zn_2SnO_4 nanoparticles) on a hydrothermal synthesis as a function of the energy available and the duration of the synthesis. From reference [43].

issues related with the use of seed-layers is the common residuals incorporated in the nanostructures, which are usually undesired for the applications. Also, without seed-layers the synthesis is less complex and this approach brings higher degree of freedom concerning the integration of nanostructures into devices [14, 32, 54].

3.1.2 ZTO phase transformations

Obtaining a single phase and shape of a multicomponent oxide as ZTO is highly desirable due to the different characteristic properties of each phase and shape, still by a hydrothermal synthesis is a challenging process as shown in the last section. In addition, the proper identification of the different possible phases obtained is a difficult task.

As previously presented, ZTO can grow in two different structural phases: Zn_2SnO_4 and $ZnSnO_3$ (fcc, orth and rhombohedral). Their identification by XRD analysis is challenging since both phases and intermediary compounds show very similar diffraction patterns. While the fcc- $ZnSnO_3$ (ICDD 00-011-0274) has a similar pattern to that of the intermediate phase $ZnSn(OH)_6$ (ICDD 01-073-2384), the orth- $ZnSnO_3$ (ICDD 00-028-1486) pattern can be confused with that of a mixture of Zn_2SnO_4 and SnO_2 . In fact, the 00-028-1486 card was deleted from the ICDD database for this reason. **Figure 4** shows the XRD peaks of these phases. For clarification, the orth- $ZnSnO_3$ identification was performed by peak indexation, using both treor and dicvol methods, for which the determined crystalline structure was proven to be orthorhombic [32].

As previously stated, temperature conditions can induce different phase transformations. For instance, Bora *et al.* studied the phase transformation of fcc- $ZnSnO_3$ nanocubes into the inverse spinel Zn_2SnO_4 through Raman analysis during *in-situ* annealing treatment [57]. In this study the phase transformation occurred at 500°C.

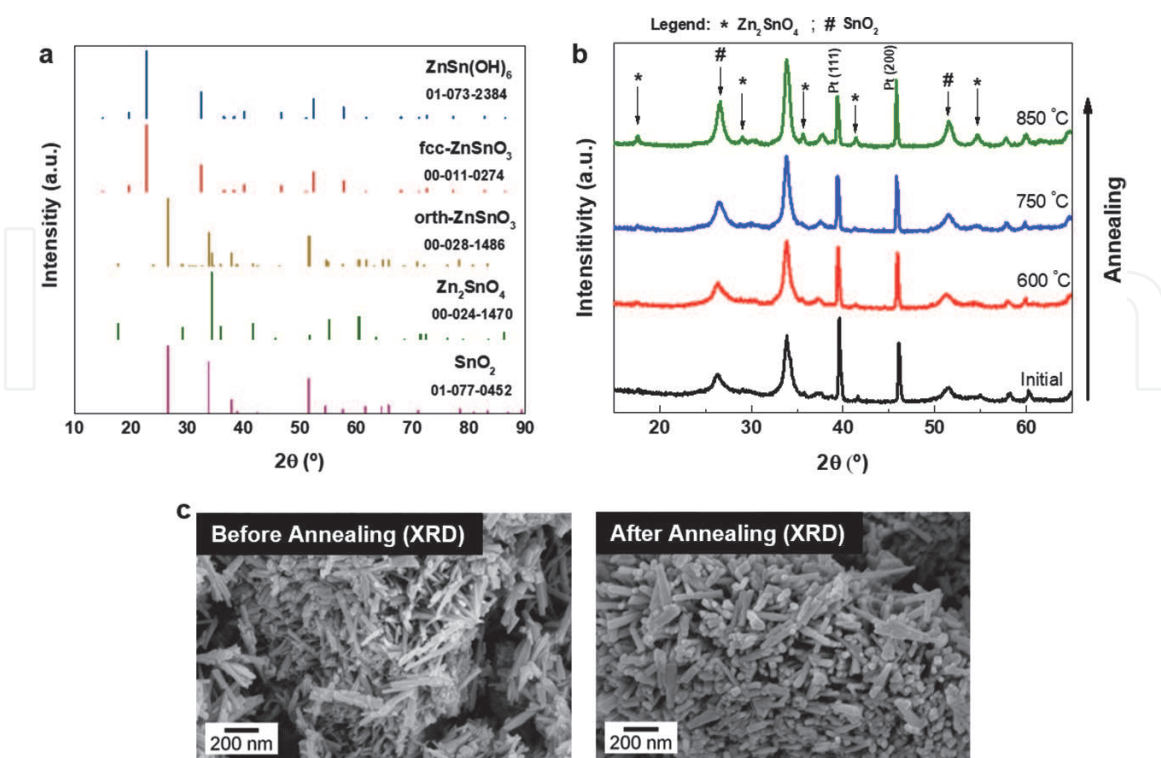


Figure 4. (a) Representation of XRD peaks of ICDD cards of: $ZnSn(OH)_6$, fcc- $ZnSnO_3$, orth- $ZnSnO_3$, Zn_2SnO_4 and SnO_2 . Note that the card 00-028-1486 (orth- $ZnSnO_3$) was deleted from ICDD. (b) In-situ XRD patterns of $ZnSnO_3$ nanowires during annealing until 850°C. (c) SEM images of the $ZnSnO_3$ nanowires before and after the in-situ annealing experiments in XRD.

Phase transformation in the ZnSnO_3 nanowires, synthesized by our group, was investigated by recording XRD patterns in the course of *in-situ* annealing treatment up to 850°C . **Figure 4b** shows the XRD patterns at different temperatures, where no phase transformation is observable below 750°C . At 850°C the characteristic peaks of Zn_2SnO_4 and SnO_2 start to be more pronounced, suggesting the phase transformation described in **Figure 3**. Nevertheless, a nanowire-like morphology is still obtained after this *in-situ* annealing experiment (**Figure 4c**), which was somehow unexpected from the experimental results used to propose the growth mechanism shown in **Figure 3**.

Thermogravimetry (TG) and differential scanning calorimetric (DSC) measurements up to 1350°C were also performed on ZnSnO_3 nanowires to shed light into this. A clear transformation occurred at $\approx 570^\circ\text{C}$ with a mass loss of $\approx 4\%$ (**Figure 5**), which can be attributed to the expected decomposition of ZnSnO_3 into Zn_2SnO_4 and SnO_2 . Through XRD patterns (**Figure 5b**) the orth- ZnSnO_3 phase is identified before the annealing, while after the annealing a predominance of SnO_2 is noticeable (mixed with Zn_2SnO_4). SEM images presented in **Figure 5c** show the nanowires before and after the annealing. After annealing, larger and rounder structures are observed for which energy dispersive X-ray spectroscopy (EDS) analysis showed a predominance of Sn (Sn/Zn ratio of 14.5), in agreement with the XRD analysis.

The difference of the decomposition temperature observed between the DSC and the XRD annealing treatments can probably be attributed to the annealing process in both techniques. While the XRD annealing is performed through the heating of a platinum foil (where the nanostructures are placed), in DSC the nanostructures are placed in a melting pot, leading to a more efficient heating and faster decomposition of the ZnSnO_3 nanowires.

These results show that when annealing processes are demanded to improve the ZnSnO_3 crystallinity, it is important to consider phase transformations carefully. Furthermore, it is noticeable that the temperatures to achieve these phase

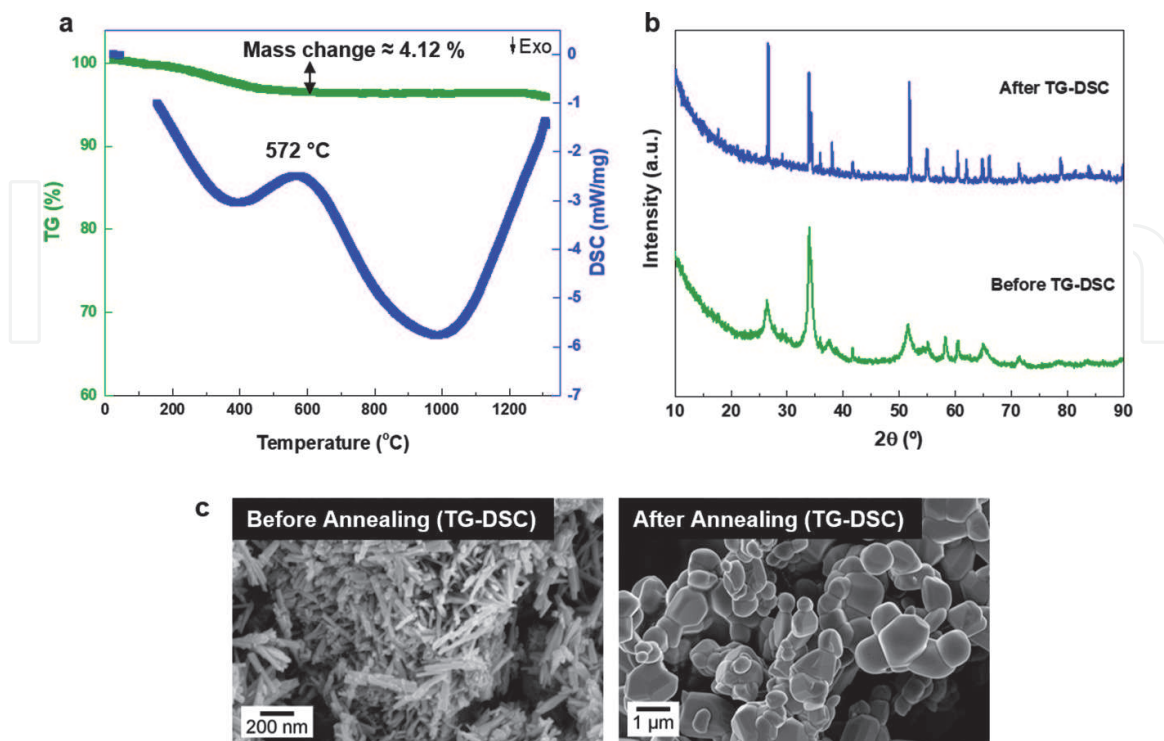


Figure 5.
(a) TG and DSC curves of as-prepared ZnSnO_3 nanowires at a heating rate of $10^\circ\text{C}/\text{min}$ at N_2 atmosphere.
(b) XRD patterns and (c) SEM images of ZnSnO_3 nanowires before and after annealing (TG-DSC measurements).

transformations as a post-synthesis treatment are significantly larger than those required during hydrothermal synthesis, owing to the higher energy provided during synthesis due to the combined effect of temperature and pressure.

3.2 Physico-chemical properties of ZTO nanostructures

The wide array of ZTO nanostructures present different physico-chemical properties which are imposed not only by the structures' shape but also by their phase (Zn_2SnO_4 or ZnSnO_3).

Concerning the optical properties, ZTO is a wide band gap semiconductor, with reported band gap values of 3.46–3.6 eV for Zn_2SnO_4 and 3.6–3.9 eV for ZnSnO_3 [18, 32, 35, 58]. Nevertheless, these values are not only dependent on the phase, but also on the shape and size of the nanostructures, with higher band gaps for smaller particles due to the quantum confinement effect [16].

While optical properties of nanostructures can be determined simply, their electrical properties are much more challenging to access, especially when considering the properties of a single nanostructure. For this reason, there are only a few reports on electrical characterization of single ZTO nanostructures. While most reports are focused on nanowires with lengths $>10\ \mu\text{m}$ (mostly produced by physical processes), smaller ZnSnO_3 nanowires (lengths $<1\ \mu\text{m}$), produced in our group by hydrothermal synthesis, were probed individually by using nanomanipulators inside SEM, as shown in **Figure 6a**. For these, an average resistivity (in vacuum) of $7.80 \pm 8.63\ \text{k}\Omega\cdot\text{cm}$ was achieved [32, 59]. When compared to the $\approx 73\ \Omega\cdot\text{cm}$ reported by Xue *et al.* for ZnSnO_3 nanowires produced by thermal evaporation (990°C), this resistivity is significantly higher [60], which can be attributed to the higher defect density expected for lower temperature (200°C) and solution-based processes. Concerning Zn_2SnO_4 nanowires, Karthik *et al.* reported a resistivity of $6\ \Omega\cdot\text{cm}$ in vacuum for nanowires synthesized by vapor phase methods at 900°C [61]. Moreover, for Zn_2SnO_4 nanostructures, which are an n-type semiconductor, mobilities higher than $112\ \text{cm}^2\text{V}^{-1}\ \text{s}^{-1}$ have already been reported, highlighting the relevance of using this material for electronic applications [62].

The ZnSnO_3 phase is well-known for its piezoelectric properties. A piezoelectric polarization along the c-axis of $\approx 59\ \mu\text{C}/\text{cm}^2$ was reported by Inaguma *et al.* for ZnSnO_3 , being much higher than the $\approx 5\ \mu\text{C}/\text{cm}^2$ reported for ZnO [64, 65]. Moreover, the piezoelectric constants of individual ZnSnO_3 and ZnO nanowires produced by hydrothermal synthesis were recently determined by piezoresponse force microscopy (PFM) measurements as $23\ \text{pm}/\text{V}$ and $9\ \text{pm}/\text{V}$, respectively

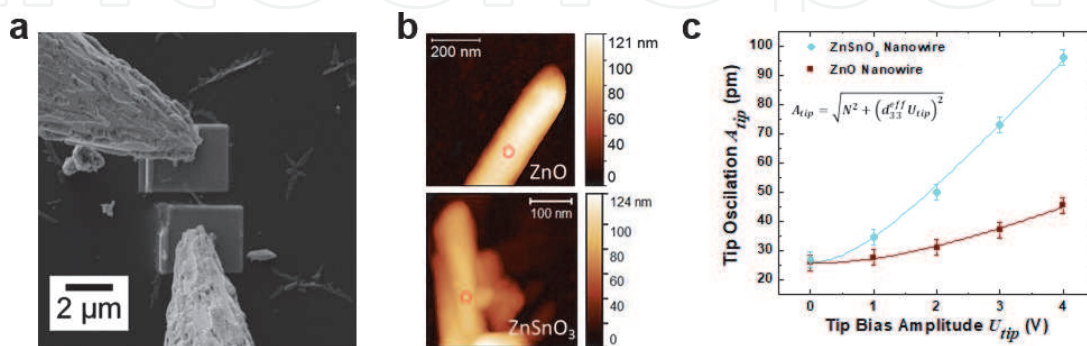


Figure 6.

(a) SEM image showing the tungsten tips of the nanomanipulators, which are contacting in-situ deposited Pt electrodes for the electrical characterization of a single ZnSnO_3 nanowire. Atomic force microscopy characterization of individual ZnO and ZnSnO_3 nanowires: (b) topographies in noncontact mode, and (c) contact mode tip oscillation as a function of tip-bias ac-voltage. Reprinted with permission from [63]. Copyright 2020 American Chemical Society.

(Figure 6b and c) [63]. The enhanced piezoelectric properties reported for ZnSnO₃ are related with the higher displacement of the Zn atom in the ZnO₆ octahedral cell when compared to the one of the Sn atom in the SnO₆ octahedral cell, leading to a higher polarization along the c-axis [66]. Even when compared with other 1D nanostructures produced by hydrothermal synthesis, only the piezoelectric constant of the well-known BaTiO₃ (31.1 pm/V) and LiNbO₃ (25 pm/V) exceeds the value reported for ZnSnO₃. Having sustainability in mind, ZnSnO₃ is then a very good alternative to both BaTiO₃ and LiNbO₃ as these contain critical raw materials [63].

Table 1 summarizes the optical, electrical, and piezoelectric properties of some of the most typical oxide semiconductor nanostructures. These properties show the potential of ZTO compared with other binary and ternary compounds to achieve the desired multifunctionality to meet the concepts of IoT and smart surfaces while avoiding the use of critical raw materials.

3.3 Application of ZTO nanostructures

The multicomponent nature, together with the wide range of different ZTO nanostructures provide this material system with truly impressive multifunctionality, which will be briefly covered next, mostly focusing on photocatalysis, energy harvesting and electronic applications.

3.3.1 Photocatalysis and piezo(photo)catalysis

Industrial actions and human activities play a negative environmental impact, raising water pollution [80]. Oxide nanostructured materials present great advantages for breakdown of water pollutants, as their band gaps are close to the visible light range and they have high surface-to-volume ratios [81]. Moreover, multicomponent oxides such as ZTO have a higher stability in aqueous environments when compared with binary compounds, which is significantly advantageous for photocatalytic applications [82].

The mechanism of photocatalytic activity of ZTO under UV light can be represented by the equations below [14, 54, 83]:



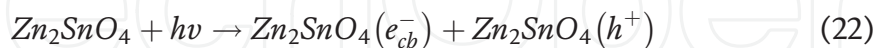
Properties Material	Band gap (eV)	Resistivity (Ω·cm)	Piezoelectric constant or polarization	References
SnO ₂	3.60	2.17	n/a	[67]
TiO ₂	3.00–3.40	1.09	n/a	[68, 69]
ZnO	3.37	1.4–2 × 10 ⁻⁴ *	5 nC/cm ² , 9–26.7 pm/V	[63, 70–72]
IGZO	3.67	>10 ⁶ –10 ⁻³ *	n/a	[73–75]
BaTiO ₃	3.47	6.25 × 10 ⁹ –2.33 × 10 ⁸	31.1 pm/V	[76–79]
ZnSnO ₃	3.90	73–1.4 × 10 ³	59 nC/cm ² , 23 ± 4 pm/V	[18, 32, 60, 63]
Zn ₂ SnO ₄	3.30–3.70	1.6	n/a	[18, 58]

The properties marked with * are referent to the bulk materials. Abbreviations: n/a – not applicable.

Table 1. Optical, electrical and piezoelectric properties of some of the most typical oxide semiconductor nanostructures.



Considering photocatalytic activity under visible light, Jain *et al.* [84] proposes the following equations:



Zn_2SnO_4 nanocrystals were used for the degradation of 50% of reactive red 141 dye in 270 min under sunlight [85]. Different $ZnSnO_3$ structures such as nanowires and nanoplates were already used as photocatalysts for organic pollutants (for example, methylene blue and rhodamine B) [33, 40, 86]. Due to its high optical band gap (3.3–3.9 eV) UV light is usually required to photoactivate this material. Nevertheless, fcc- $ZnSnO_3$ nanoparticles were already reported with a very satisfactory photocatalytic behavior on methylene blue degradation under visible light ($0.0156\ min^{-1}$) [81].

Alternatives to the conventional photocatalytic approach have also been explored, making use of the piezoelectric properties of materials such as $ZnSnO_3$ (nanowires and nanoplates) for piezocatalysis (in the dark) [87] or for piezophotocatalysis (under illumination) [42, 87, 88]. Indeed, piezoelectricity and ferroelectricity (associated with perovskite structures) have shown to play an important role in photocatalysis, since the photogeneration of electron–hole pairs is enhanced by the dipole moment formed by the polarization electric field across polar materials [89, 90]. A schematic representation of the piezocatalytic mechanism is presented in **Figure 7b** and shows the influence of the characteristic polarization of the piezoelectric materials, which contributes to the generation of hydroxyl radicals and consequently degradation of rhodamine B. The dye degradation was achieved in 2.5 h, with a degradation rate of $4.5 \times 10^{-2}\ min^{-1}$ [87].

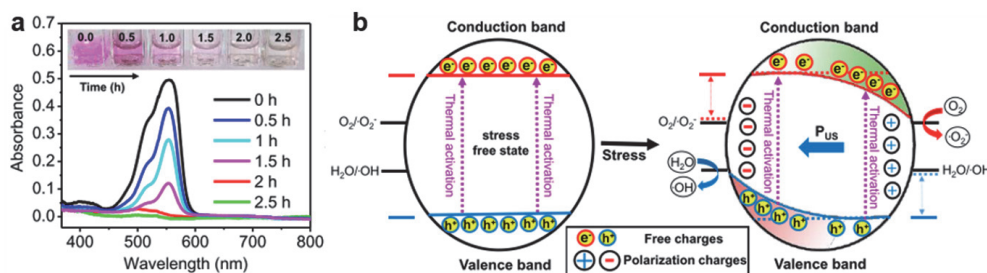


Figure 7. (a) Piezocatalysis using $ZnSnO_3$ nanoparticles under ultrasound exposure. (b) Schematic of the piezocatalytic mechanism. Reprinted with permission from [87]. Copyright (2020) American Chemical Society.

Other interesting applications of photocatalytic properties have been reported, such as the photocatalytic inactivation of *Escherichia coli* using ZTO nanocubes under visible light. Only a 10% surviving rate was found for the bacteria, whereas the absorption of the visible light was attributed to the inherent surface defects enhancing the absorption edge in the visible region [82]. With this in mind, lower cost methods for nanostructure production (as hydrothermal methods), which typically result in more defective structures, might be advantageous for these applications as defect levels near the band edges may increase the absorption for lower energy levels.

3.3.2 Piezoelectric energy harvesting with ZTO nanostructures

Nanogenerators are devices that can convert external stimulus into electrical energy, being highly interesting for smart and self-sustainable surfaces, as they can be used for sustainable energy sources, biomedical systems and smart sensors [91]. Due to its excellent ferroelectric and piezoelectric properties, different ZnSnO_3 nanostructures (i.e., nanowires, nanoplates, nanocubes) have been widely explored for energy harvesting devices and sensitive human motion sensors, through their piezoelectric (induction of electrical charge by the applied mechanical strain) and piezoresistive (electrical resistivity change by the applied mechanical strain) effects, respectively [45, 66, 92–94]. The fcc- ZnSnO_3 nanocubes have been the most popular ZTO structures for these applications. For instance, Wang *et al.* reported the nanogenerators of fcc- ZnSnO_3 nanocubes mixed with polydimethylsiloxane (PDMS), reaching a maximum output of 400 V, 28 μA at a current density of $7 \mu\text{A}\cdot\text{cm}^{-2}$ [95]. While, Paria *et al.* mixed fcc- ZnSnO_3 nanocubes with polyvinyl chloride (PVC), achieving a maximum output of ≈ 40 V and $\approx 1.4 \mu\text{A}$, corresponding to a power density of $3.7 \mu\text{W}\cdot\text{cm}^{-3}$ (Figure 8a) [94].

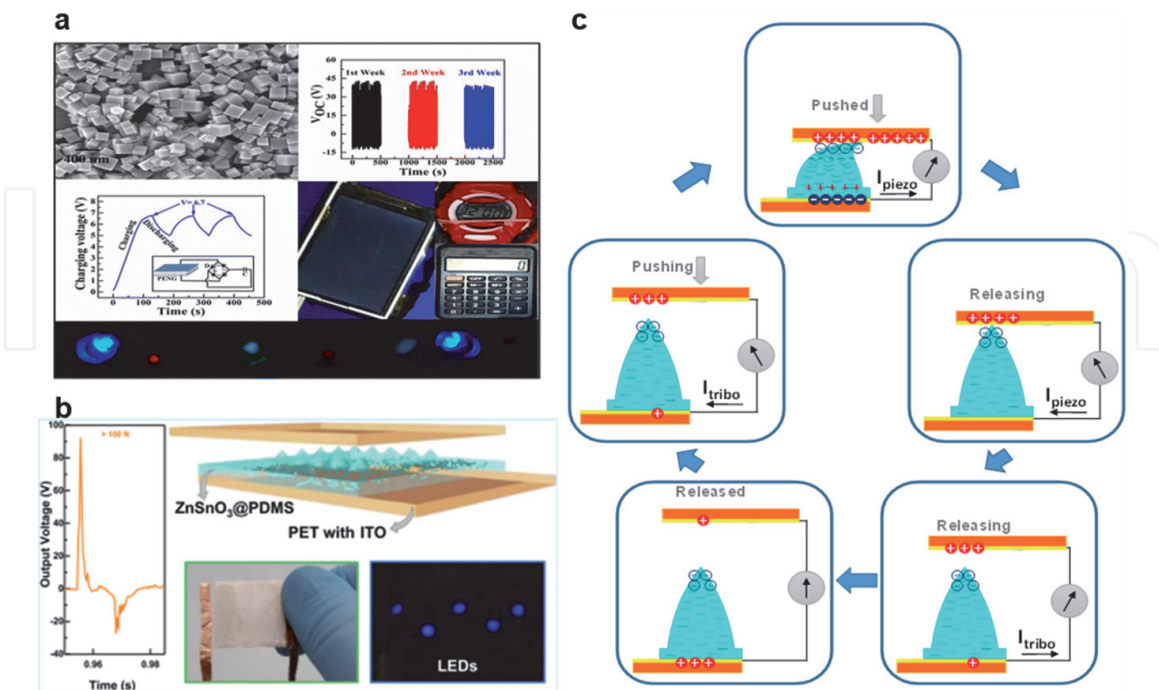


Figure 8. Hybrid nanogenerators of: (a) a composite film based on fcc- ZnSnO_3 nanocubes and PVC. Reprinted with permission from [94], copyright 2020 American Chemical Society; and (b) a composite film based on orth- ZnSnO_3 nanowires and PDMS. (c) Schematic of the charge generation mechanism in the micro-structured devices of (b). Images (b) and (c) were reprinted with permission from [63], copyright 2020 American Chemical Society.

ZnSnO₃ nanoplates were also applied for nanogenerators. Guo *et al.* reported produced nanogenerators fabricated with orth-ZnSnO₃ nanoplates embedded in flat films of PDMS, reaching voltage and current outputs of 20 V and 0.6 μA, respectively, under bending stress [45]. More recently in our group, orth-ZnSnO₃ nanowires were mixed with PDMS to fabricate nanogenerators of micro-structured composites (**Figure 8b**) [63]. In the same work, a charge generation and displacement mechanism was proposed, as depicted in **Figure 8c**. Briefly, the micro-structures induced in PDMS are suggested to improve the force delivery to the nanowires, enhancing its piezoelectric signal, while bringing also a triboelectric contribution to the nanogenerator output. This results in an output voltage, current and instantaneous power of approximately 9 V, 1 μA and 3 μW·cm⁻², respectively, when applying a force of only 10 N. For higher forces the devices were capable to reach outputs around 120 V and 13 μA, which was shown to be enough energy to light up LEDs and several small electronic devices [63].

3.3.3 Electronic applications

Electronic applications are always a relevant drive for materials. Multicomponent semiconductor nanostructures as ZTO are particularly interesting for these applications, with wide band gap semiconductors allowing for high-power and high-frequency operations [50]. Field-effect transistors (FETs) are the key elements enabling today's electronics, being 1D nanostructures particularly interesting in this regard, given the easiness of confining migratory direction of charge carriers through its length, i.e., between source and drain electrodes. Indeed, 1D nanostructures have already proven great usefulness for the upcoming generations of semiconductors in FETs [96]. While several reports already demonstrated ZTO as a candidate for replacement of IGZO in thin film technologies [13], similarly, ZTO is also one of the most promising multicomponent metal oxides for transistors with nanostructures [62]. Demonstrations of discrete Zn₂SnO₄ nanotransistors have already been made using nanotransfer molding of ZTO inks followed by annealing at 500°C, or by simple pick-and-place approach of drop-casted ZTO nanowires prepared by CVD above 700°C and by thermal evaporation at 1000°C [39, 97, 98]. While the achievement of on/off ratio ≈10⁶ and field-effect mobility ≈20 cm²/Vs is a good demonstration of the ZTO's potential, transistors using ZTO nanostructures synthesized by solution processes have not been reported yet. Furthermore, these nanostructures have also been used for the resistive switch layer in the emerging type of memory devices known as memristors. Reports show ZTO as the active material in memristors in the form of both Zn₂SnO₄ nanowires and ZnSnO₃ nanocubes, being the latter especially relevant for this application due to its ferroelectric properties. Properties such as high off/on ratios (>10⁵), long retention times (>5 months) and fast response speeds (<20 ns) are obtained for these devices [99, 100].

Transforming ZTO or other nanostructures into well-established LAE semiconductor materials, while highly desirable from the performance and functionality point of view, will still require significant advances in reliable techniques for alignment and density control in transparent (and flexible) substrates [101].

3.3.4 Other applications

Besides the applications briefly presented above, ZTO nanostructures have also been widely used in sensing applications, with gas sensors being the most popular [102]. Their small crystallite size, high surface-to-volume ratios and surface reactivity result in enhanced sensitivities/selectivity, with multicomponent materials

typically presenting smaller response times and superior stabilities compared to binary compounds [103]. Moreover, the implementation of these nanostructures in sensors allows miniaturization of the devices, as well as cost reduction. ZnSnO₃ has been reported as an excellent humidity sensor, in different nanostructure forms such as nanoparticles or even in composites of ZnSnO₃ nanocubes and Ag nanowires [29, 104]. Additionally, ZnSnO₃ nanoparticles were used as electrochemical biosensors for label free sub-femtomolar detection of cardiac biomarker troponin T and a composite of Zn₂SnO₄ nanoparticles and graphene was used for morphine and codeine detection [105, 106]. Recently, Durai *et al.* reported ultra-selective sensors, based on ZnSnO₃ nanocubes modified glassy carbon electrode (GCE), for simultaneous detection of uric acid and dopamine through differential pulse voltammetry technique [107]. Zn₂SnO₄ and ZnSnO₃ nanostructures of different shapes such as nanoparticles, nanowires and nanocubes, have also been widely explored as photoconductors [23, 108–111]. While the optical band gap of these materials is typically in the UV energy levels (hence their transparency in visible range), quantum confinement effects or even defect levels near the band edges can be explored to increase the absorption for lower energy levels. Other applications that have been explored using ZTO nanostructures are related with energy storage and conversion. Zn₂SnO₄ has been widely used as photoanode for dye solar cells in different nanostructure morphologies such as nanoparticles and nanowires [21, 35]. Cherian *et al.* reported the performance of nanowires and compared with nanoplates of Zn₂SnO₄ for Li-batteries [34]. Supercapacitors (SC) have also started to be explored using ZTO nanostructures, with Bao *et al.* having reported the use of Zn₂SnO₄/MnO₂ core shell in carbon fibers showing a capacitance of 621.6 F·g⁻¹ [112].

4. Conclusions

Expanding LAE to IoT and smart surface concepts requires an increasing number of objects to have embedded electronics, sensors and connectivity, driving a demand for compact, smart, multifunctional and self-sustainable technology with low associated costs. While nanomaterials are thought to be able to meet these requirements, playing an important role in the future technological world, low cost and sustainable technologies are demanded. For this, both low cost fabrication methods and sustainable materials must be considered. This chapter shows the versatility of the hydrothermal method to control the growth and morphology of zinc tin oxide (ZTO) nanostructures, and the variety of shapes that can be produced for each of the different ZTO phases. Compared to other preparation methods, especially vapor phase methods, hydrothermal synthesis reveals a large set of advantages from both research and industrial viewpoints. First, while the multitude of parameters to control requires an in-depth understanding of their role in the final products, it also brings enormous flexibility to tune the synthesis process for the desired results. Also, it can be performed at low temperature (< 200°C), which is compatible with a wide range of substrates for direct growth, while assuring lower costs. This links perfectly with the demonstrated upscaling capability of hydrothermal synthesis which is a crucial aspect for industrial implementation.

Furthermore, a summary of exciting results that have been reported regarding application in devices of these ZTO nanostructures over the past few years is presented. The multifunctionality of this material system is highlighted by its successful implementation in energy harvesters, photocatalysis, electronic devices, sensors, and others.

Acknowledgements

The authors would like to thank Ana Pimentel for the TG-DSC measurement.

This work is funded by FEDER funds through the COMPETE 2020 Programme and National Funds through the FCT – Fundação para a Ciência e a Tecnologia, I.P., under the scope of the project UIDB/50025/2020, and the doctoral grant research number SFRH/BD/131836/2017. This work also received funding from the European Community's H2020 program under grant agreement No. 716510 (ERC-2016-StG TREND), No. 787410 (ERC-2018-AdG DIGISMART) and No. 685758 (1D-Neon). This work is part of the PhD Thesis in Nanotechnologies and Nanosciences defended by Ana Rovisco at FCT-NOVA entitled "Solution-based Zinc Tin oxide nanostructures: from synthesis to applications" in December 2019.

Conflict of interest

The authors declare no conflict of interest.

Author details

Ana Isabel Bento Rovisco*, Rita Branquinho, Joana Vaz Pinto, Rodrigo Martins, Elvira Fortunato and Pedro Barquinha*

CENIMAT/i3N, Department of Materials Science, NOVA School of Science and Technology (FCT-NOVA) and CEMOP/UNINOVA, NOVA University Lisbon, Campus de Caparica, Caparica, Portugal

*Address all correspondence to: a.rovisco@fct.unl.pt and pmcb@fct.unl.pt

IntechOpen

© 2020 The Author(s). Licensee IntechOpen. This chapter is distributed under the terms of the Creative Commons Attribution License (<http://creativecommons.org/licenses/by/3.0>), which permits unrestricted use, distribution, and reproduction in any medium, provided the original work is properly cited. 

References

- [1] Mancini L, Sala S, Recchioni M, Benini L, Goralczyk M, Pennington D. Potential of life cycle assessment for supporting the management of critical raw materials. *Int J Life Cycle Assess.* 2015;20: 100–16.
- [2] Flexible, Printed and Organic Electronics 2019–2029: Forecasts, Players & Opportunities: IDTechEx. 2020.
- [3] He Y, Wang X, Gao Y, Hou Y, Wan Q. Oxide-based thin film transistors for flexible electronics. *J Semicond.* 2018;39(1).
- [4] Martins J, Bahubalindrani P, Rovisco A, Kiazadeh A, Martins R, Fortunato E, et al. Bias Stress and Temperature Impact on InGaZnO TFTs and Circuits. *Materials (Basel).* 2017;10(12):680.
- [5] Fortunato E, Barquinha P, Martins R. Oxide semiconductor thin-film transistors: a review of recent advances. *Adv Mater.* 2012;24(22):2945–86.
- [6] Bahubalindrani PG, Kiazadeh A, Sacchetti A, et al. Influence of Channel Length Scaling on InGaZnO TFTs Characteristics: Unity Current-Gain Cutoff Frequency, Intrinsic Voltage-Gain, and On-Resistance. *J Disp Technol.* 2016;12(6):515–8.
- [7] Baraton M-I. The Future of TCO Materials: Stakes and Challenges. *MRS Proc.* 2009;1209:1209-P03–06.
- [8] European Commission. COMMUNICATION FROM THE COMMISSION TO THE EUROPEAN PARLIAMENT, THE COUNCIL, THE EUROPEAN ECONOMIC AND SOCIAL COMMITTEE AND THE COMMITTEE OF THE REGIONS. 2020.
- [9] Theerthagiri J, Salla S, Senthil RA, Nithyadharseni P, Madankumar A, Arunachalam P, Maiyalagan, T, Kim, H-S. A review on ZnO nanostructured materials: Energy, environmental and biological applications. *Nanotechnology.* 2019;30:392001.
- [10] Baskoutas S. Special Issue: Zinc Oxide Nanostructures: Synthesis and Characterization. *Materials (Basel).* 2018;11(6):873.
- [11] Shankar KS, Raychaudhuri AK. Fabrication of nanowires of multicomponent oxides: Review of recent advances. *Mater Sci Eng C.* 2005; 25(5–8):738–51.
- [12] Facchetti A, Marks TJ, Wiley InterScience (Online service). *Transparent electronics : from synthesis to applications.* Wiley; 2010. 448 p.
- [13] Fernandes C, Santa A, Santos Â, Bahubalindrani P, Deuermeier J, Martins R, et al. A Sustainable Approach to Flexible Electronics with Zinc-Tin Oxide Thin-Film Transistors. *Adv Electron Mater.* 2018;4(7):1800032.
- [14] Baruah S, Dutta J. Zinc stannate nanostructures: hydrothermal synthesis. *Sci Technol Adv Mater.* 201;12:013004.
- [15] Rabenau A. The Role of Hydrothermal Synthesis in Preparative Chemistry. *Angew Chemie Int Ed English.* 1985;24(12):1026–40.
- [16] Annamalai A, Carvalho D, Wilson KC, Lee M-J. Properties of hydrothermally synthesized Zn₂SnO₄ nanoparticles using Na₂CO₃ as a novel mineralizer. *Mater Charact.* 2010;61: 873–81.
- [17] Pimentel A, Ferreira S, Nunes D, Calmeiro T, Martins R, Fortunato E. Microwave Synthesized ZnO Nanorod Arrays for UV Sensors: A Seed Layer Annealing Temperature Study. *Materials (Basel).* 2016;9(4):299.

- [18] Miyauchi M, Liu Z, Zhao Z-G, Anandan S, Hara K. Single crystalline zinc stannate nanoparticles for efficient photo-electrochemical devices. *Chem Commun.* 2010;46:1529–31.
- [19] Sun S, Liang S. Morphological zinc stannate: synthesis, fundamental properties and applications. *J Mater Chem A.* 2017;5:20534–60.
- [20] Lehnen T, Zopes D, Mathur S. Phase-selective microwave synthesis and inkjet printing applications of Zn₂SnO₄ (ZTO) quantum dots. *J Mater Chem.* 2012;22(34):17732.
- [21] Tan B, Toman E, Li Y, Wu Y. Zinc Stannate (Zn₂SnO₄) Dye-Sensitized Solar Cells. *J Am Chem Soc.* 2007;129:4162–3.
- [22] Joseph LA, Jeronsia JE, Jaculine MM, Das SJ. Investigations on Structural and Optical Properties of Hydrothermally Synthesized Zn₂SnO₄ Nanoparticles. *Phys Res Int.* 2016;2016:1–6.
- [23] Wang YF, Ding Y, Zhao JS, Wang X, Li DJ, Li XF. Optimized Zn₂SnO₄ nanoparticles with enhanced performance for photodetectors and photocatalysts. *RSC Adv.* 2016;6(73):69191–5.
- [24] Dimitrievska M, Ivetić TB, Litvinchuk AP, Fairbrother A, Miljević BB, Štrbac GR, et al. Eu³⁺-Doped Wide Band Gap Zn₂SnO₄ Semiconductor Nanoparticles: Structure and Luminescence. *J Phys Chem C.* 2016;120(33):18887–94.
- [25] Šepelák V, Becker SM, Bergmann I, Indris S, Scheuermann M, Feldhoff A, et al. Nonequilibrium structure of Zn₂SnO₄ spinel nanoparticles. *J Mater Chem.* 2012;22(7):3117.
- [26] Wu YS, Chang WK, Jou M. Photocatalytic Analysis and Characterization of Zn₂SnO₄ Nanoparticles Synthesized via Hydrothermal Method with Na₂CO₃ Mineralizer. *Adv Mater Res.* 2010;97–101:19–22.
- [27] Sun G, Zhang S, Li Y. Solvothermal Synthesis of Zn₂SnO₄ Nanocrystals and Their Photocatalytic Properties. *Int J Photoenergy.* 2014;2014:1–7.
- [28] Jia T, Liu M, Yu D, Long F, Mo S, Deng Z, et al. A Facile Approach for the Synthesis of Zn₂SnO₄/BiOBr Hybrid Nanocomposites with Improved Visible-Light Photocatalytic Performance. *Nanomaterials.* 2018;8(5):313.
- [29] Singh R, Yadav AK, Gautam C. Synthesis and Humidity Sensing Investigations of Nanostructured ZnSnO₃. *J Sens Technol.* 2011;01(04):116–24.
- [30] Modeshia DR, Walton RI. Solvothermal synthesis of perovskites and pyrochlores: crystallisation of functional oxides under mild conditions. *Chem Soc Rev.* 2010;39(11):4303.
- [31] Mageshwari K, Kim TG, Park J. Effect of alkaline concentration on the structural and luminescence properties of ZnSnO₃ nanoparticles obtained by facile reflux method. *J Mater Sci Mater Electron.* 2016;27(4):4093–7.
- [32] Rovisco A, Branquinho R, Martins J, Oliveira MJ, Nunes D, Fortunato E, et al. Seed-Layer Free Zinc Tin Oxide Tailored Nanostructures for Nanoelectronic Applications: Effect of Chemical Parameters. *ACS Appl Nano Mater.* 2018;1(8):3986–97.
- [33] Beshkar F, Amiri O, Salehi Z. Synthesis of ZnSnO₃ nanostructures by using novel gelling agents and their application in degradation of textile dye. *Sep Purif Technol.* 2017;184:66–71.
- [34] Cherian CT, Zheng M, Reddy M V, Chowdari BVR, Sow CH. Zn₂SnO₄ Nanowires versus Nanoplates: Electrochemical Performance and

- Morphological Evolution during Li-Cycling. *ACS Appl Mater Interfaces*. 2013;5(13):6054–60.
- [35] Li Z, Zhou Y, Bao C, Xue G, Zhang J, Liu J, et al. Vertically building Zn₂SnO₄ nanowire arrays on stainless steel mesh toward fabrication of large-area, flexible dye-sensitized solar cells. *Nanoscale*. 2012;4:3490–4.
- [36] Zhou T, Liu X, Zhang R, Wang Y, Zhang T. Shape control and selective decoration of Zn₂SnO₄ nanostructures on 1D nanowires: Boosting chemical-sensing performances. *Sensors Actuators B Chem*. 2019;290:210–6.
- [37] Chen Z, Cao M, Hu C. Novel Zn₂SnO₄ hierarchical nanostructures and their gas sensing properties toward ethanol. *J Phys Chem C*. 2011;115:5522–9.
- [38] Xue XY, Chen YJ, Wang YG, Wang TH. Synthesis and ethanol sensing properties of ZnSnO₃ nanowires. *Appl Phys Lett*. 2005;86:1–3.
- [39] Pang C, Yan B, Liao L, Liu B, Zheng Z, Wu T, et al. Synthesis, characterization and opto-electrical properties of ternary Zn₂SnO₄ nanowires. *Nanotechnology*. 2010;21:465706.
- [40] Fang C, Geng B, Liu J, Zhan F. d-fructose molecule template route to ultra-thin ZnSnO₃ nanowire architectures and their application as efficient photocatalyst. *Chem Commun*. 2009;(17):2350.
- [41] Men H, Gao P, Zhou B, Chen Y, Zhu C, Xiao G, et al. Fast synthesis of ultra-thin ZnSnO₃ nanorods with high ethanol sensing properties. *Chem Commun*. 2010;46:7581.
- [42] Lo M-K, Lee S-Y, Chang K-S. Study of ZnSnO₃-Nanowire Piezophotocatalyst Using Two-Step Hydrothermal Synthesis. *J Phys Chem C*. 2015;119(9):5218–24.
- [43] Rovisco A, Branquinho R, Martins J, Fortunato E, Martins R, Barquinha P. Growth Mechanism of Seed-Layer Free ZnSnO₃ Nanowires: Effect of Physical Parameters. *Nanomaterials*. 2019;9(7):1002.
- [44] Joseph J, Saseendran SB, Achary SR, Sukumaran AA, Jayaraj MK. Zinc stannate flakes for optoelectronic and antibacterial applications. *Dae Solid State Physics Symposium 2018*. 2019. p. 030026.
- [45] Guo R, Guo Y, Duan H, Li H, Liu H. Synthesis of Orthorhombic Perovskite-Type ZnSnO₃ Single-Crystal Nanoplates and Their Application in Energy Harvesting. *ACS Appl Mater Interfaces*. 2017;9(9):8271–9.
- [46] Chen Y, Yu L, Li Q, Wu Y, Li Q, Wang T. An evolution from 3D face-centered-cubic ZnSnO₃ nanocubes to 2D orthorhombic ZnSnO₃ nanosheets with excellent gas sensing performance. *Nanotechnology*. 2012;23(41):415501.
- [47] Wang Y, Gao P, Bao D, Wang L, Chen Y, Zhou X, et al. One Pot, Two Phases: Individual Orthorhombic and Face-Centered Cubic ZnSnO₃ Obtained Synchronously in One Solution. *Inorg Chem*. 2014;53(23):12289–96.
- [48] Ji X, Huang X, Liu J, Jiang J, Li X, Ding R, et al. Hydrothermal synthesis of novel Zn₂SnO₄ octahedron microstructures assembled with hexagon nanoplates. *J Alloys Compd*. 2010;503:L21–5.
- [49] Jie J, Wang G, Han X, Fang J, Yu Q, Liao Y, et al. Growth of Ternary Oxide Nanowires by Gold-Catalyzed Vapor-Phase Evaporation. *J Phys Chem B*. 2004;108:8249–53.
- [50] Zhou Z, Lan C, Wei R, Ho JC. Transparent metal-oxide nanowires and their applications in harsh electronics. *J Mater Chem C*. 2019;7(2):202–17.

- [51] Einarsrud M-A, Grande T. 1D oxide nanostructures from chemical solutions. *Chem Soc Rev.* 2014;43(7):2187–99.
- [52] Kumari V, Patra AK, Bhaumik A. Self-assembled ultra-small zinc stannate nanocrystals with mesoscopic voids via a salicylate templating pathway and their photocatalytic properties. *RSC Adv.* 2014;4:13626–34.
- [53] Fu X, Wang X, Long J, Ding Z, Yan T, Zhang G, et al. Hydrothermal synthesis, characterization, and photocatalytic properties of Zn₂SnO₄. *J Solid State Chem.* 2009;182(3):517–24.
- [54] Zeng J, Xin M, Li, Wang H, Yan H, Zhang W. Transformation Process and Photocatalytic Activities of Hydrothermally Synthesized Zn₂SnO₄ Nanocrystals. *J Phys Chem C.* 2008;112(11):4159–67.
- [55] Guerfi Y, Larrieu G. Vertical Silicon Nanowire Field Effect Transistors with Nanoscale Gate-All-Around. *Nanoscale Res Lett.* 2016;11(1):210.
- [56] Barrocas B, Sérgio S, Rovisco A, Melo Jorge M. Visible-Light Photocatalysis in Ca_{0.6}Ho_{0.4}MnO₃ Films Deposited by RF-Magnetron Sputtering Using Nanosized Powder Compacted Target. *J Phys Chem C.* 2014;118(1):590–7.
- [57] Bora T, Al-Hinai MH, Al-Hinai AT, Dutta J. Phase Transformation of Metastable ZnSnO₃ Upon Thermal Decomposition by In-Situ Temperature-Dependent Raman Spectroscopy. *J Am Ceram Soc.* 2015;98(12):4044–9.
- [58] Lei M, Sheng Y, Wan L, Bi K, Huang K, Jia R, et al. A novel self-catalytic route to zinc stannate nanowires and cathodoluminescence and electrical transport properties of a single nanowire. *J Alloys Compd.* 2016; 657:394–9.
- [59] Rovisco A. Solution-based Zinc-Tin Oxide nanostructures : from synthesis to applications [PhD Thesis]. Universidade NOVA de Lisboa; 2019.
- [60] Xue XY, Chen YJ, Li QH, Wang C, Wang YG, Wang TH. Electronic transport characteristics through individual ZnSnO₃ nanowires. *Appl Phys Lett.* 2006;88(18):182102.
- [61] Karthik KRG, Andreasson BP, Sun C, Pramana SS, Varghese B, Sow CH, et al. Physical and Electrical Properties of Single Zn₂SnO₄ Nanowires. *Electrochem Solid-State Lett.* 2011;14:K5.
- [62] Kim S, Kim H, Janes DB, Ju S. Interface studies of N₂ plasma-treated ZnSnO nanowire transistors using low-frequency noise measurements. *Nanotechnology.* 2013;24:305201.
- [63] Rovisco A, dos Santos A, Cramer T, Martins J, Branquinho R, Águas H, et al. Piezoelectricity Enhancement of Nanogenerators Based on PDMS and ZnSnO₃ Nanowires through Microstructuration. *ACS Appl Mater Interfaces.* 2020;12(16):18421–30.
- [64] Inaguma Y, Yoshida M, Katsumata T. A Polar Oxide ZnSnO₃ with a LiNbO₃-Type Structure. *J Am Chem Soc.* 2008;130(21):6704–5.
- [65] Dal Corso A, Posternak M, Resta R, Baldereschi A. Ab initio study of piezoelectricity and spontaneous polarization in ZnO. *Phys Rev B.* 1994; 50:10715–21.
- [66] Wu JM, Xu C, Zhang Y, Yang Y, Zhou Y, Wang ZL. Flexible and transparent nanogenerators based on a composite of lead-free ZnSnO₃ triangular-belts. *Adv Mater.* 2012;24(45):6094–9.
- [67] Hernández-Ramírez F, Tarancón A, Casals O, Rodríguez J, Romano-Rodríguez A, Morante JR, et al. Fabrication and electrical characterization of circuits based on

- individual tin oxide nanowires. *Nanotechnology*. 2006;17:5577–83.
- [68] Nunes D, Pimentel A, Santos L, Barquinha P, Fortunato E, Martins R. Photocatalytic TiO₂ Nanorod Spheres and Arrays Compatible with Flexible Applications. *Catalysts*. 2017;7(2):60.
- [69] Fàbrega C, Hernández-Ramírez F, Daniel Prades J, J. On the photoconduction properties of low resistivity TiO₂ nanotubes. *Nanotechnology*. 2010;21(44).
- [70] Pimentel A, Samouco A, Nunes D, Araújo A, Martins R, Fortunato E. Ultra-Fast Microwave Synthesis of ZnO Nanorods on Cellulose Substrates for UV Sensor Applications. *Materials (Basel)*. 2017;10(11):1308.
- [71] Ellmer K. Resistivity of polycrystalline zinc oxide films: Current status and physical limit. *J Phys D Appl Phys*. 2001;34(21):3097–108.
- [72] Zhao M, Wang Z, Mao SX. Piezoelectric Characterization of Individual Zinc Oxide Nanobelt Probed by Piezoresponse Force Microscope. *Nano Lett*. 2004;4(4):587–90.
- [73] Santos L, Nunes D, Calmeiro T, Branquinho R, Salgueiro D, Barquinha P, et al. Solvothermal Synthesis of Gallium–Indium–Zinc–Oxide Nanoparticles for Electrolyte-Gated Transistors. *ACS Appl Mater Interfaces*. 2015;7(1):638–46.
- [74] Barquinha P, Pereira L, Gonçalves G, Martins R, Fortunato E. Toward High-Performance Amorphous GIZO TFTs. *J Electrochem Soc*. 2009;156(3):H161.
- [75] Zan H-W, Tsai W-W, Chen C-H, Tsai C-C, Meng H-F. 4.3: High Performance a-IGZO TFT with Nano-Dots Doping. *SID Symp Dig Tech Pap*. 2011;42(1):28–31.
- [76] Tang H, Zhou Z, Sodano HA. Large-scale synthesis of Ba_xSr_{1-x}TiO₃ nanowires with controlled stoichiometry. *Appl Phys Lett*. 2014;104(14):142905.
- [77] Huang X, Xie L, Jiang P, Wang G, Liu F. Electrical, thermophysical and micromechanical properties of ethylene-vinyl acetate elastomer composites with surface modified BaTiO₃ nanoparticles. *J Phys D Appl Phys*. 2009;42(24).
- [78] Salehi H, Shahtahmasebi N, Hosseini SM. Band structure of tetragonal BaTiO₃. *Eur Phys J B*. 2003;32(2):177–80.
- [79] Suzuki K, Kijima K. Optical band gap of barium titanate nanoparticles prepared by RF-plasma chemical vapor deposition. *Japanese J Appl Physics*. 2005;44(4 A):2081–2.
- [80] Kampouri S, Stylianou KC. Dual-Functional Photocatalysis for Simultaneous Hydrogen Production and Oxidation of Organic Substances. *ACS Catal*. 2019;9(5):4247–70.
- [81] Najam Khan M, Al-Hinai M, Al-Hinai A, Dutta J. Visible light photocatalysis of mixed phase zinc stannate/zinc oxide nanostructures precipitated at room temperature in aqueous media. *Ceram Int*. 2014;40:8743–52.
- [82] Khan MN, Jaisai M, Dutta J. Photocatalytic Inactivation of *Escherichia coli* Using Zinc Stannate Nanostructures under Visible Light. *Adv Mater Res*. 2015;1131:203–9.
- [83] Tatarchuk T, Peter A, Al-Najar B, Vijaya J, Bououdina M. Photocatalysis: Activity of Nanomaterials. *Nanotechnology in Environmental Science*. 2018. 209–92.
- [84] Jain S, Shah AP, Shimpi NG. An efficient photocatalytic degradation of organic dyes under visible light using

- zinc stannate (Zn_2SnO_4) nanorods prepared by microwave irradiation. *Nano-Structures & Nano-Objects*. 2020; 21:100410.
- [85] Foletto EL, Simões JM, Mazutti M a., Jahn SL, Muller EI, Pereira LSF, et al. Application of Zn_2SnO_4 photocatalyst prepared by microwave-assisted hydrothermal route in the degradation of organic pollutant under sunlight. *Ceram Int*. 2013;39(4): 4569–74.
- [86] Borhade A V., Baste YR. Study of photocatalytic asset of the $ZnSnO_3$ synthesized by green chemistry. *Arab J Chem*. 2017;10:S404–11.
- [87] Biswas A, Saha S, Jana NR. $ZnSnO_3$ Nanoparticle-Based Piezocatalysts for Ultrasound-Assisted Degradation of Organic Pollutants. *ACS Appl Nano Mater*. 2019;2(2):1120–8.
- [88] Wang Y-T, Chang K-S. Piezopotential-Induced Schottky Behavior of $Zn_{1-x}SnO_3$ Nanowire Arrays and Piezophotocatalytic Applications. Xie R-J, editor. *J Am Ceram Soc*. 2016;99(8):2593–600.
- [89] Chen F, Huang H, Guo L, Zhang Y, Ma T. The Role of Polarization in Photocatalysis. *Angew Chemie Int Ed*. 2019;58(30):10061–73.
- [90] Liang Z, Yan CF, Rtimi S, Bandara J. Piezoelectric materials for catalytic/ photocatalytic removal of pollutants: Recent advances and outlook. *Appl Catal B Environ*. 2019;241:256–69.
- [91] Askari H, Khajepour A, Khamesee MB, Saadatnia Z, Wang ZL. Piezoelectric and triboelectric nanogenerators: Trends and impacts. *Nano Today*. 2018;22(1):10–3.
- [92] Alam MM, Ghosh SK, Sultana A, Mandal D. Lead-free $ZnSnO_3$ /MWCNTs-based self-poled flexible hybrid nanogenerator for piezoelectric power generation. *Nanotechnology*. 2015;26(16):165403.
- [93] Choi KH, Siddiqui GU, Yang B, Mustafa M. Synthesis of $ZnSnO_3$ nanocubes and thin film fabrication of ($ZnSnO_3$ /PMMA) composite through electrospray deposition. *J Mater Sci Mater Electron*. 2015;26:5690–6.
- [94] Paria S, Karan SK, Bera R, Das AK, Maitra A, Khatua BB. A Facile Approach To Develop a Highly Stretchable PVC/ $ZnSnO_3$ Piezoelectric Nanogenerator with High Output Power Generation for Powering Portable Electronic Devices. *Ind Eng Chem Res*. 2016;55(40):10671–80.
- [95] Wang G, Xi Y, Xuan H, Liu R, Chen X, Cheng L. Hybrid nanogenerators based on triboelectrification of a dielectric composite made of lead-free $ZnSnO_3$ nanocubes. *Nano Energy*. 2015;18:28–36.
- [96] Liu Z, Xu J, Chen D, Shen G. Flexible electronics based on inorganic nanowires. *Chem Soc Rev*. 2015;44(1): 161–92.
- [97] Hwang JK, Cho S, Dang JM, Kwak EB, Song K, Moon J, et al. Direct nanoprinting by liquid-bridge-mediated nanotransfer moulding. *Nat Nanotechnol*. 2010;5:742–8.
- [98] Lim T, Kim H, Meyyappan M, Ju S. Photostable Zn_2SnO_4 Nanowire Transistors for Transparent Displays. *ACS Nano*. 2012;6(6):4912–20.
- [99] Dong H, Zhang X, Zhao D, Niu Z, Zeng Q, Li J, et al. High performance bipolar resistive switching memory devices based on Zn_2SnO_4 nanowires. *Nanoscale*. 2012;4(8):2571–4.
- [100] Siddiqui GU, Rehman MM, Choi KH. Enhanced resistive switching in all-printed, hybrid and flexible memory device based on perovskite

- ZnSnO₃ via PVOH polymer. *Polymer (Guildf)*. 2016;100:102–10.
- [101] Nunes D, Pimentel A, Santos L, Barquinha P, Pereira L, Fortunato E, et al. Metal oxide nanostructures: Synthesis, properties and applications. Elsevier; 2018. 1–328 p.
- [102] Chen Q, Wang Y, et al. Enhanced acetone sensor based on Au functionalized In-doped ZnSnO₃ nanofibers synthesized by electrospinning method. *J Colloid Interface Sci*. 2019;543:285–99.
- [103] Wan, Sun J, Liu H. Semiconducting Oxide Nanowires: Growth, Doping and Device applications. *Nanowires - Implementations and Applications*. InTech; 2011. p. 59–98.
- [104] Sharma A, Kumar Y, Shirage PM. Structural, optical and excellent humidity sensing behaviour of ZnSnO₃ nanoparticles: effect of annealing. *J Mater Sci Mater Electron*. 2018;29(13):10769–83.
- [105] Supraja P, Sudarshan V, Tripathy S, Agrawal A, Singh SG. Label free electrochemical detection of cardiac biomarker troponin T using ZnSnO₃ perovskite nanomaterials. *Anal Methods*. 2019;11(6):744–51.
- [106] Bagheri H, Khoshsafar H, Afkhami A, Amidi S. Sensitive and simple simultaneous determination of morphine and codeine using a Zn₂SnO₄ nanoparticle/graphene composite modified electrochemical sensor. *New J Chem*. 2016;40(8):7102–12.
- [107] Durai L, Badhulika S. One pot hydrothermal synthesis of large area nano cube like ZnSnO₃ perovskite for simultaneous sensing of Uric Acid and Dopamine using differential pulse voltammetry. *IEEE Sens J*. 2020;1748 (c):1–1.
- [108] Dong Y, Wang S, Zou Y, Liu S, Zhu Z, Li J, et al. Zinc Stannate Nanocrystal-Based Ultrarapid-Response UV Photodetectors. *Adv Mater Technol*. 2018;3(6):1800085.
- [109] Zhang Y, Wang J, et al. High performance ultraviolet photodetectors based on an individual Zn₂SnO₄ single crystalline nanowire. *J Mater Chem*. 2010;20(44):9858.
- [110] Zhao Y, Hu L, Liu H, Liao M, Fang X, Wu L. Band Gap Tunable Zn₂SnO₄ Nanocubes through Thermal Effect and Their Outstanding Ultraviolet Light Photoresponse. *Sci Rep*. 2015;4(1):6847.
- [111] Xue XY, Guo TL, Lin ZX, Wang TH. Individual core-shell structured ZnSnO₃ nanowires as photoconductors. *Mater Lett*. 2008;62 (8–9):1356–8.
- [112] Bao L, Zang J, Li X. Flexible Zn₂SnO₄/MnO₂ Core/Shell Nanocable–Carbon Microfiber Hybrid Composites for High-Performance Supercapacitor Electrodes. *Nano Lett*. 2011;11(3):1215–20.